The Nature of Electronic Contact in Self-Assembled Monolayers for Molecular Electronics: Evidence for Strong Coupling

ARTICLE *in* THE JOURNAL OF PHYSICAL CHEMISTRY B · OCTOBER 1999

Impact Factor: 3.3 · DOI: 10.1021/jp9916337

3 AUTHORS, INCLUDING:

Christopher J Cramer
University of Minnesota Twin Cities
532 PUBLICATIONS **23,458** CITATIONS

The Nature of Electronic Contact in Self-Assembled Monolayers for Molecular Electronics: Evidence for Strong Coupling

T. Vondrak, C. J. Cramer, and X.-Y. Zhu*

Department of Chemistry and Super Computer Institute, University of Minnesota, Minneapolis, Minnesota 55455

Received: May 19, 1999; In Final Form: August 16, 1999

Self-assembled-monolayers (SAMs) of aromatic thiolates on metal surfaces are candidates for molecular "quantum dots" or "wires". We probe the interfacial electronic structure using two-photon photoemission in SAMs of pentafluorothiophenolate ($C_6F_5S^-$) on Cu(111). Compared to gas-phase C_6F_5SH, the σ^* LUMO in the assembled molecule is stabilized by 3.1 eV and the HOMO−LUMO gap is reduced by 5.7 eV. Ab initio calculations reveal that stabilization of molecular states is, to a great extent, a consequence of the strong electronic coupling between metal and molecular orbitals via the −S− bridge. This strong electronic coupling is absent when the molecule is not directly bonded to the surface, as in the case of C_6F_6 weakly adsorbed on Cu(111).

1. Introduction

The use of a single molecule as a "quantum dot" or "quantum wire" in charge transport has attracted considerable attention due to its exciting potential in future electronic devices. This excitement is evident in the observation of Coulomb blockade and the demonstration of a room-temperature single electron transistor in carbon nanotubes.[1,2] An attractive alternative to carbon nanotubes is the use of organic molecules, such as conjugated oligomers and aromatic molecules, as single electron transport devices. This is because the easy incorporation of functional groups and the availability of a large repertoire of synthetic techniques facilitates the rational design and assembly of molecular electronic devices. A number of groups have studied the electron transport in single molecules using thiol self-assembled monolayers (SAMs) on gold surfaces.[3−6] For example, Reed et al. measured electron transport in benzene-1,4-dithiol (HSC_6H_4SH) self-assembled onto two adjacent Au electrodes of a mechanically controllable break junction and suggested the possibility of Coulomb blockade.[4] Using scanning tunneling microscopy (STM), Dhirani et al. found a rectifying effect in a SAM of conjugated $C_6H_5C{\equiv}CC_6H_4C{\equiv}CC_6H_4SH$ on Au.[5] Datta and co-workers measured the current−voltage characteristics in STM for α,α′-xylyl dithiol ($HSCH_2C_6H_4CH_2$-SH) self-assembled on Au;[6] in particular, they compared experiment with simulation based on the scattering theory of transport and showed the strong dependence of current−voltage characteristics on the relative alignment of molecular states with metal Fermi levels, on the spatial profile of the electrostatic potential, and on the relative distance of the STM tip to the molecule.

A critical issue in interpreting experimental current−voltage measurements and in designing self-assembled monolayers of molecular electronics is understanding the interfacial electronic structure and the electronic coupling between molecular orbitals and the metal substrate. While the importance of this issue has certainly been realized by most researchers[3−6] and received attention in recent theoretical studies,[7−9] there has been little experimental effort aimed at directly probing the interfacial electronic structure in self-assembled monolayer systems. As a result, much confusion remains about the electronic nature of the −S−metal contact and little is known about the extent of electronic interaction between the conjugated molecular framework and the metal surface. It is the purpose of the present study to systematically establish the interfacial electronic structure in a SAM of molecular electronics using laser two-photon photoemission (2PPE) spectroscopy in conjunction with electronic structural calculations. The experimental approach is illustrated schematically in Figure 1. Two-photon photoemission can be used to characterize both occupied and unoccupied electronic states, such as the highest occupied molecular orbital (HOMO) and the lowest unoccupied molecular orbital (LUMO). To characterize the former, coherent two-photon excitation (dashed arrows) from the occupied state below the Fermi level leads to the ejection of one electron. This is similar to conventional one-photon photoemission, except that the change in electron kinetic energy (ΔE_{kin}) scales with twice that of photon energy, i.e., $\Delta E_{kin} = 2\Delta h\nu$. To identify the LUMO, the absorption of one photon (solid arrow) creates hot substrate electrons that can tunnel to an unoccupied molecular state; the absorption of a second photon (solid arrow) excites this transient electron above the vacuum level. In this case, ΔE_{kin} scales with $1\Delta h\nu$. One of the most exciting prospects of 2PPE is that it can be carried out in a time-resolved manner using femtosecond laser pulses to directly probe the ultrafast electron dynamics involving the LUMO state. 2PPE has been used successfully in characterizing the energetics and dynamics of image states on metal surfaces.[10−12] The use of 2PPE in characterizing adsorbate resonances and dynamics has also been reported.[13−15]

The system we examine is a self-assembled monolayer (SAM) of pentafluorothiophenolate, $C_6F_5S^-$, on Cu(111), shown schematically in the lower left of Figure 1. This system is compared to perfluorobenzene weakly adsorbed in the second molecular layer on Cu(111) (lower right), as characterized recently in our laboratory.[16] We use fluorobenzenes as model molecular electronic components because their electronic structures are

* To whom correspondence should be addressed. E-mail: zhu@chem.umn.edu. Fax: (612) 626-7541.

10.1021/jp9916337 CCC: $18.00
Published on Web 09/30/1999

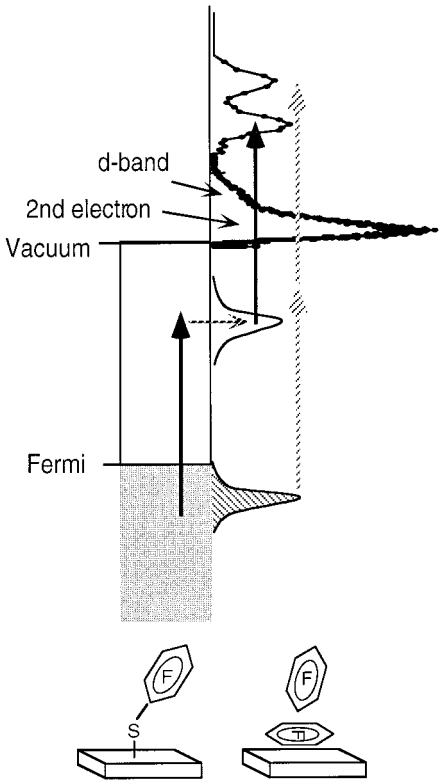

Figure 1. Schematic illustration of characterizing HOMO and LUMO in adsorbed molecules by two-photon photoemission spectroscopy. The lower part shows the two chemical systems: pentafluorothiophenolate (C_6F_5S) SAM on Cu(111) and bilayer perfluorobenzene on Cu(111).

well-known from extensive studies in both the gas and condensed phases.[17,18] Cu(111) is selected since recent 2PPE studies on adsorbates have been mainly carried out on this surface and they serve as useful points of reference.[13−15]

We found that, for the fluorobenzene group attached to Cu via the −S− linker in the self-assembled monolayer, the molecular LUMO is stabilized by more than 3 eV and the HOMO−LUMO gap is decreased by 5.7 eV as compared to gas-phase pentafluorothiophenol. These large changes in orbital energy cannot be accounted for exclusively by stabilization of anionic and cationic states due to polarization effects. Instead, the majority of the stabilization energy must come from direct, strong electronic coupling between the substrate and the adsorbate. Ab initio calculations on model molecules confirm this conclusion. This kind of strong electronic coupling is absent when the fluorobenzene molecule is located at a similar distance, but weakly coupled to the Cu surface, as in C_6F_6 on Cu(111).

2. Experimental Section

All experiments were performed in an ultrahigh vacuum (UHV) chamber detailed elsewhere.[16] A 30 cm long electron time-of-flight (TOF) spectrometer was used for 2PPE spectroscopy. Electrons were detected by multichannel plates and recorded by a multichannel scaler with 5 ns resolution. Laser light for 2PPE was from a YAG-pumped dye laser (Continuum). The UV output (290−330 nm, 5 ns pulse width) was passed through an iris (1 mm i.d.) and a quartz window and directed at the sample surface at 60° from surface normal. The electric field of the incident light was at 45° from the plane of incidence. The reflected light exited the UHV chamber through a UV window. All measurements reported here were recorded with the sample normal to the center axis of the TOF tube and at a sample temperature of 300 K. A low laser pulse energy density

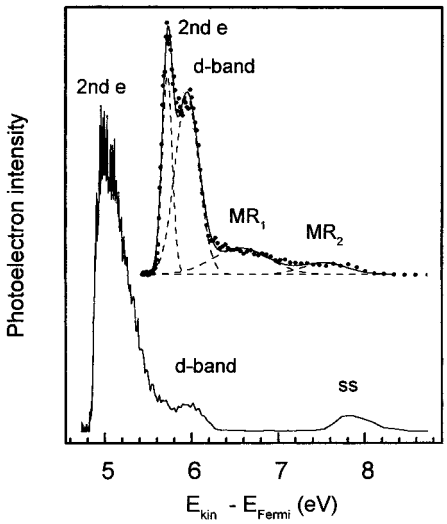

Figure 2. Two-photon photoemission spectra obtained for a self-assembled monolayer of C_6F_5S/Cu(111), top, and clean Cu(111), bottom, at a photon energy of 4.13 eV. The dashed curves on the upper spectrum are from deconvolutions assuming Gaussian peak shapes and the solid curve is the sum of dashed curves. Dots are experimental data points. ss: surface state. MR: molecular resonances.

of 1−3 mJ/cm^2 was used to avoid space charge problems. The Cu(111) sample was cleaned by Ar^+ sputtering and annealing to yield a sharp (1 × 1) low-energy-electron-diffraction pattern. The cleanness is further confirmed by Auger electron spectroscopy.

Pentafluorothiophenol, C_6F_5SH (Aldrich), was purified by freeze−pump−thaw cycles. The self-assembled monolayer was formed by dosing C_6F_5SH onto the Cu(111) surface at a substrate temperature of 300 K, with total exposure exceeding 10^4 Langmuir (L). This leads to a completely saturated surface. Recent studies of alkanethiol SAMs on Au(111) showed the formation of the saturated 2D crystalline phase at gas exposures $\geq 2 \times 10^3$ L, while less dense phases (2D liquid and gas) were formed at lower exposures.[19] Although the majority of studies have concentrated on Au(111),[20] thiol SAMs have been shown also to form on Cu(111).[20,21] Thiophenolate is known to form SAM on metal surfaces.[22−25] Despite the lack of long range order, each $C_6H_5S−$ is believed to be oriented with a tilt angle of ∼25° from surface normal.[25] The adsorption of pentafluorothiophenol on Pt(111) also results in the formation of densely packed thiophenolate monolayers with uniform orientation, presumably with the phenyl ring closely aligned with surface normal.[26,27] In view of the above studies, we expect similar SAMs to form on Cu(111) from pentafluorothiophenolate.

3. Results and Discussions

3.1. Determination of HOMO and LUMO Levels by 2PPE. Figure 2 compares the 2PPE spectrum of a self-assembled monolayer of C_6F_5S/Cu(111) with that from clean Cu(111) taken at $h\nu = 4.13$ eV. The spectrum from the clean surface is characterized by three peaks: the peak labeled SS originates from an occupied surface state located at 0.4 eV below the Fermi level, while the two peaks at lower energy are assigned to the Cu d-band (d) and secondary electrons (second e).[10−16] When the Cu(111) surface is covered with the SAM, the surface state is eliminated, in agreement with previous studies on chemisorption.[13,14] The spectrum consists of four peaks: the intense secondary electron and d-band peaks at low energies and two broad and overlapping peaks above 6.3 eV. We assign the new features above the d-band peak to photoemission due to

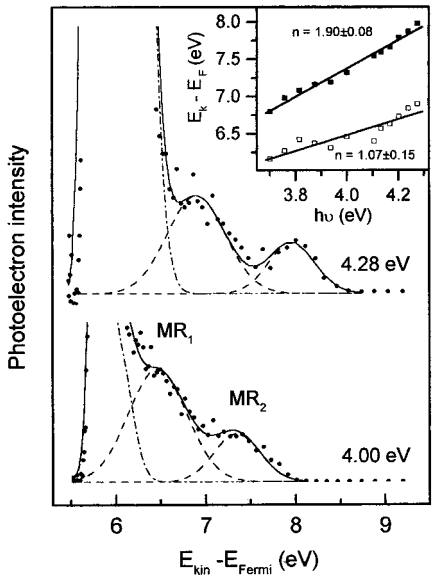

Figure 3. Two representative 2PPE spectra from the SAM-covered surface taken at $h\nu = 4.0$ and 4.28 eV. Each spectrum is scaled to show only regions of molecular resonances. The dashed curves derive from Gaussian deconvolution of the two molecular peaks. The inset shows the peak positions for MR_1 (open squares) and MR_2 (solid squares) as a function of photon energy. The solid lines are least-squares linear fits which yield the indicated slopes (n).

assembled molecules. Assuming Gaussian peak shapes, we can deconvolute the spectrum from the SAM-covered surface into four peaks (dashed curves). The deconvolution of the broad molecular feature into two peaks (labeled MR_1 and MR_2) is justified because they are partially resolved, particularly at high photon energies, as detailed later in Figure 3. Note that, compared to the clean surface, the onset of the secondary electron peak from the SAM-covered surface is 0.7 eV higher, indicating an increase in the surface work function. Thus, the work function of the SAM-covered surface is 5.6 eV, based on a value of 4.9 eV for clean Cu(111).[13] In the following, we focus on the broad peak from SAM-covered surface and analyze its dependence on photon energy.

Figure 3 shows two representative spectra from the SAM-covered surface taken at $h\nu = 4.0$ and 4.28 eV. Each spectrum is scaled to show only regions of molecular resonances. The dashed curves derive from Gaussian deconvolution of the two molecular peaks. In the deconvolution procedure, we used fixed peak widths for all spectra taken at different photon energies (fwhm = 0.8 eV for MR_1 and 0.6 eV for MR_2). The positions of these two peaks shift with increasing photon energy, but at different rates. The deconvolution results are summarized in the inset, where the data points are peak positions and the solid lines are least-squares linear fits. These fits yield slopes of $n = 1.07 \pm 0.15$ and 1.90 ± 0.08 for MR_1 and MR_2, respectively. Within experimental uncertainty, these slopes are essentially 1 and 2, respectively. Thus, the two peaks in 2PPE spectra from the SAM of C_6F_5S/Cu(111) originate from (i) the transfer of a photoexcited substrate electron to an unoccupied molecular state between the Fermi and the vacuum level, followed by photoionization of this transient anionic molecular state, and (ii) coherent two photon excitation from an occupied molecular state below the Fermi level. On the basis of photon energies and electron kinetic energies, we found that the unoccupied state is located at −3.2 eV and the occupied state at −6.4 eV (referenced to the vacuum level). We assign these two molecular states to the lowest unoccupied molecular orbital (LUMO) and the highest occupied molecular orbital (HOMO), respectively.

TABLE 1: Vertical IP and EA Values for C_6F_5SX and Partial Charges (σ) by Group/Atom in the Anionic State

C_6F_5SX	IP, eV	EA, eV	σ (C_6F_5)	σ (S)	σ (X)
X = H	8.98	0.06	−0.54	−0.42	−0.03
X = Li	7.78	0.73	−0.33	−0.67	0.00
X = Cu	8.04	1.43	−0.23	−0.26	−0.51

3.2. Computation of Model Molecules. The gas-phase electronic structure of C_6F_5SH is not well established experimentally, but related molecules, such as pentafluorobenzene (C_6F_5H) and perfluorobenzene (C_6F_6), have been extensively studied.[17,18] To further interpret HOMO and LUMO energies in the gas phase, we have carried out ab initio calculations on three model systems: 2,3,4,5,6-pentafluorothiophenol (**1**), lithium 2,3,4,5,6-pentafluorothiophenoxide (**2**), and copper(I) 2,3,4,5,6-pentafluorothiophenoxide (**3**). All geometries were fully optimized at the B3LYP level of electronic structure theory,[28,29] using basis sets 6-31G* for Li,[30] cc-pVDZ for C, F, and S,[31,32] and the all-electron polarized double-ζ basis set of Schafer et al. for Cu.[33] These basis sets will hereafter be referred to generically as pVDZ. All three optimized structures were verified as local minima by calculation of analytical force constants.

Vertical ionization potentials (IP) and electron affinities (EA) were computed as differences in energies between neutrals and radical cations and radical anions, respectively, at the geometries of the neutral species. For these single point calculations, the basis sets employed were 6-31+G* for Li[30,34−36] and aug-cc-pVDZ for C, F, and S,[31,32] and for Cu the basis set of Schafer and co-workers was augmented with one set each of diffuse s, p, and d functions having exponents of 0.009, 0.042, and 0.100, respectively.[33] These basis sets will hereafter be referred to generically as pVDZ+.

Computed gas-phase ionization potentials and electron affinities at the pVDZ+//pVDZ level are presented in Table 1. Also shown in Table 1 is the distribution of partial charge (σ) in the anionic state, which will be discussed later. In every case, the electronic state of the radical cation is $^2A''$ and that of the radical anion is $^2A'$. That is, the ionizing electron derives from the aromatic π system while the captured electron goes into the σ framework. To evaluate the ability of this level of theory and basis sets to accurately predict EA values, we computed the EA of perfluorobenzene (which has been experimentally determined also to have a $^2A'$ ground state). The predicted value of 0.04 eV is in excellent agreement with the experimental value of ∼0.0 eV.[17] Note that this EA value should not be confused with the adiabatic EA corresponding to a relaxed $C_6F_6^-$.[18] More thorough evaluations of B3LYP/large basis set calculations have found EA and IP values computed at this level to be accurate to within 0.2 eV for a wide range of molecules.

3.3. Nature of Electronic Coupling. HOMO and LUMO levels determined in 2PPE experiments are essentially those of transient cations and anions, respectively. Thus, these energy levels and the corresponding HOMO−LUMO gap are substantially different from those involved in the optical transition of a neutral system. Instead, we should compare the HOMO and LUMO levels to the vertical EA and IP values obtained in the above calculation, as shown schematically in Figure 4. Compared to gas-phase **1**, the LUMO in the SAM on Cu(111) is lowered by 3.1 eV. We can identify at least four contributions to the stabilization of a negative ion state in the self-assembled monolayer: (i) polarization of surrounding molecules, (ii) charge-image attraction, (iii) lateral delocalization of molecular orbitals in band formation, and (iv) direct electronic interaction (wave function mixing) with the substrate.

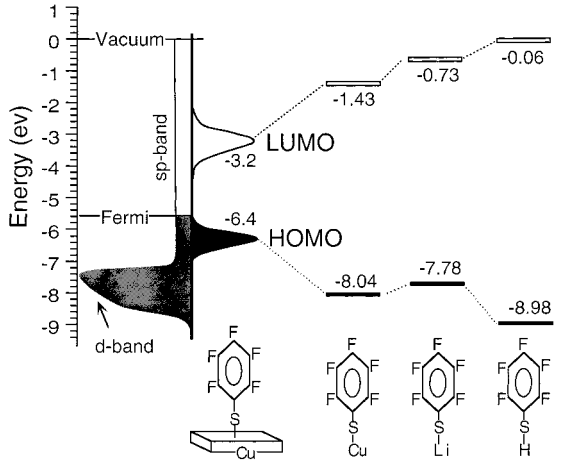

Figure 4. Energy level diagram showing the positions of HOMO and LUMO levels in the SAM of C_6F_5S/Cu(111) and in gas-phase molecules, C_6F_5SX (X = Cu, Li, H). Also shown on the left is the approximate Cu bulk band structure.

Effect i is well-known in the condensed phase. For example, the relaxed $C_6F_6^-$ state involving the σ^* level is believed to be 0.4 eV more stable in condensed phases than in the gas phase, a result of solvation.[18] Considering the two-dimensional nature of the self-assembled monolayer, we expect the effective stabilization by surrounding molecules in the SAM to be less than 0.4 eV.

Stabilization of a negative ion state by the charge-image attraction potential, i.e., effect ii, is given in atomic units by $-\mathrm{Ry}/(2\kappa z)$, where Ry is the Rydberg constant, z is the distance of the charge from the image plane, and κ is the permittivity. We can approximate the image plane by the metal surface, κ by the vacuum permittivity, and the position of the charge by the center of the pentafluorophenyl group. Using the geometry obtained in a recent molecular dynamics simulation for C_6H_5S/Au(111),[25] we estimate that the pentafluorophenyl ring in C_6F_5S/Cu(111) should be approximately at a distance of 3.5−4 Å from the surface plane. This corresponds to a stabilization energy of ∼1.0 eV.

Additional stabilization is possible if the LUMO level is delocalized laterally due to intermolecular electronic coupling, effect iii. However, angle-resolved 2PPE measurement for C_6F_5S/Cu(111) showed no measurable change in the peak positions for both MR_1 and MR_2 with increasing detection angle (data not shown). Thus, there is no measurable dispersion and both LUMO and HOMO in adsorbed C_6F_5S must be fairly localized.

Taking the maximum estimated values for the above effects, we believe that stabilization of the negative ion state in the SAM due to direct wave function mixing between the adsorbed molecule and the metal surface, i.e., effect iv, should account for at least 1.7 eV. Thus, there must be strong mixing between the molecular LUMO and substrate electronic structures (through the S atom). The strong electronic coupling between the molecular LUMO and the metal substrate is supported by our computational results for metal pentafluorothiophenolates: going from C_6F_5SH to C_6F_5SLi and C_6F_5SCu, the LUMO decreases from −0.06 eV to −0.73 and −1.43 eV, respectively. The physical reason for this trend is obvious. From H to Li and Cu, an increasing number of diffuse atomic orbitals become available in the valence energy region. These diffuse atomic orbitals help to delocalize the extra charge on the anionic molecule. In this regard, the S atom is an effective "conducting" bridge between the molecule and the metal atom, because of the availability of atomic orbitals on this bridge that hybridize well (i.e., conduct) with both the aromatic ring and the bonded metals. As a further illustration of this point, we have calculated partial atomic charges by atom or group for the anionic LUMO state in the C_6F_5SX (X = H, Li, Cu) system, as summarized in Table 1. While there is almost no extra charge on H or Li, over 50% of the extra charge is localized on the Cu atom in the $C_6F_5SCu^-$ molecule. This kind of delocalization should only increase when C_6F_5S- is bonded to the full Cu(111) surface.

The same argument applies to the increase in the π HOMO level upon metal substitution. We believe the positive hole is stabilized due to screening by increased electron density on the metal atom and/or the S bridge, as well as direct wave function mixing. This is in addition to the charge-image potential and solvation effect due to surrounding molecules in the self-assembled monolayer.

The strong electronic coupling effect is not observed when the molecule is not directly bonded to the surface. Recently, we carried out a 2PPE study of perfluorobenzene (C_6F_6) adsorbed on Cu(111).[16] We found that the σ^* LUMO in adsorbed C_6F_6 is stabilized by 1.8 eV, as compared to the gas-phase vertical EA. This effect can be largely attributed to the charge-image potential and solvation effect due to surrounding molecules.[16]

It is important to point out that, while the HOMO is a π state, as expected from a mixture of the aromatic ring with the Cu d-state via the S atom, the LUMO is a σ^* state, not the π^* state. In long molecular "wires", the unoccupied level that participates in conduction should be the delocalized π^* state. This delocalized π^* state within the conjugated molecular framework cannot couple to the σ^* LUMO at the interface for symmetry reasons. Thus, in the energy range when π^* is mainly responsible for electron transport, the interfacial σ^* LUMO may behave as a barrier. This issue is the focus of an ongoing study in our laboratory.[37]

4. Conclusions

We have used two-photon photoemission to successfully establish the interfacial electronic structure in a model self-assembled monolayer system, pentafluorothiophenolate, $C_6F_5S^-$, on Cu(111). We found that, relative to the vacuum, the highest occupied molecular orbital (HOMO) is located at −6.4 eV while the lowest unoccupied molecular orbital (LUMO) is at −3.2 eV. A comparison to accurate ab initio calculations on gas-phase pentafluorothiophenol shows that the σ^* LUMO in the assembled molecule is stabilized by 3.1 eV and the HOMO−LUMO gap is decreased from 8.9 to 3.2 eV. Calculations on metal pentafluorothiophenolates C_6F_5SLi and C_6F_5SCu reveal that the stabilization of the molecular states is, to a great extent, a direct consequence of the strong electronic coupling (direct wave function mixing) between the metal substrate and the molecular orbitals via the −S− bridge. Supporting this, we found that the strong electronic coupling is absent when the molecule is not directly bonded to the surface, as in the case of C_6F_6 weakly adsorbed on Cu(111).

Acknowledgment. This work was supported by the University of Minnesota and the Super Computer Institute. X.Y.Z. acknowledges support by Research Corp. in the form of a Cottrell Scholar Award and the Petroleum Research Fund administrated by the American Chemical Society. C.J.C. acknowledges support by the Alfred P. Sloan Foundation. We thank Martin Wolf for loaning us the Cu(111) sample.

References and Notes

(1) Tans, S. J.; Devoret, M. H.; Dai, H.-J.; Thess, A.; Smalley, R. E.; Geerling, L. J.; Dekker, C. *Nature* **1997**, *386*, 474.

(2) Tans, S. J.; Verschueren, A. R. M.; Dekker, C. *Nature* **1998**, *393*, 49.

(3) Bumm, L. A.; Arnold, J. J.; Cygan, M. T.; Dunbar, T. D.; Burgin, T. P.; Jones, L.; II; Allara, D. L.; Tour, J. M.; Weiss, P. S. *Science* **1996**, *271*, 1705.

(4) Reed, M. A.; Zhou, C.; Muller, C. J.; Burgin, T. P.; Tour, J. M. *Science* **1997**, *278*, 252.

(5) Dhirani, A.-A.; Lin, P. H.; Guyot-Sionnest, P.; Zehner, R. W.; Sita, L. R. *J. Chem. Phys.* **1997**, *106*, 5249.

(6) Datta, S.; Tian, W.; Hong, S.; Reifenberger, R.; Henderson, J. I.; Kubiak, C. P. *Phys. Rev. Lett*. **1997**, *79*, 2530.

(7) Magoga, M.; Joachim, C. *Phys. Rev. B* **1998**, *57*, 1820.

(8) Yaliraki, S. Y.; Ratner, M. A. *J. Chem. Phys.* **1998**, *109*, 5036.

(9) Seminario, J. M.; Zacarias, A. G.; Tour, J. M. *J. Am. Chem. Soc.* **1999**, *121*, 411.

(10) Fauster, Th.; Steinmann, W. In *Photonic probes of surfaces*; Halevi, P., Ed.; Elsevier: Amsterdam, 1995.

(11) Harris, C. B.; Ge, N. H.; Lingle, R. L.; McNeill, J. D.; Wong, C. M. *Annu. Rev. Phys. Chem.* **1997**, *48*, 711.

(12) Hofer, U.; Shumay, I. L.; Reuss, Ch.; Thomann, U.; Wallauer, W.; Fauster, Th. *Science* **1997**, *277*, 1480.

(13) Knoesel, E.; Hertel, T.; Wolf, M.; Ertl, G. *Chem. Phys. Lett.* **1995**, *240*, 409.

(14) Bauer, M.; Pawlik, S.; Aeschlimann, M. *Phys. Rev. B* **1997**, *55*, 10040.

(15) Ogawa, S.; Nagano, H.; Petek, H. *Phys. Rev. Lett.* **1999**, *82*, 1931.

(16) Vondrak, T.; Zhu, X.-Y. *J. Phys. Chem.* **1999**, *103*, 3449.

(17) Hitchcock, A. P.; Fischer, P.; Gedanken, A.; Robin, M. B. *J. Phys. Chem.* **1987**, *91*, 531 and references therein.

(18) Christophorou, L. G.; Datskos, P. G.; Faidas, H. *J. Chem. Phys.* **1994**, *101*, 6728 and references therein.

(19) Porier, G. E.; Pylant, E. D. *Science* **1996**, *272*, 1145.

(20) Ulman, A. *Chem. Rev.* **1996**, *96*, 1533.

(21) Zamborini, F. P.; Campbell, J. K.; Crooks, R. M. *Langmuir* **1998**, *14*, 640.

(22) Chang, S.-C.; Chao, I.; Tao, Y.-T. *J. Am. Chem. Soc.* **1994**, *116*, 6792.

(23) Tao, Y.-T.; Wu, C.-C.; Eu, J.-Y.; Lin, W.-L.; Wu, K.-C.; Chen, C.-H. *Langmuir* **1997**, *13*, 4018.

(24) Dhirani, A.-A.; Zehner, R. W.; Hsung, R. P.; Guyot-Sionnest, P.; Sita, L. R. *J. Am. Chem. Soc.* **1996**, *118*, 3319.

(25) Jung, H. H.; Won, Y. D.; Shin, S.; Kim, K. *Langmuir* **1999**, *15*, 1147.

(26) Stern, D. A.; Wellner, E.; Salaita, G. N.; Laguren-Davidson, L.; Lu, F.; Batina, N.; Frank, D. G.; Zapien, D. C.; Walton, N.; Hubbard, A. T. *J. Am. Chem. Soc.* **1988**, *110*, 4885.

(27) Hayes, W. A.; Shannon, C. *Langmuir* **1996**, *12*, 3688.

(28) Becke, A. D. *J. Chem. Phys.* **1993**, *98*, 5648.

(29) Stephens, P. J.; Devlin, F. J.; Ashwar, C. S.; Bak, K. L.; Taylor, P. R.; Frisch, M. J. In *Chemical Applications of Density Functional Theory*; Laird, B. B., Ross, R. B., Ziegler, T., Eds.; American Chemical Society: Washington, DC, 1996; Vol. 629.

(30) Hariharan, P. C.; Pople, J. A. *Chem. Phys. Lett.* **1972**, 66, 217. Hariharan, P. C.; Pople, J. A. *Theor. Chim. Acta* **1973**, *28*, 213.

(31) Dunning, T. H. *J. Chem. Phys.* **1989**, *90*, 1007.

(32) Woon, D. E.; Dunning, T. H. *J. Chem. Phys.* **1993**, *98*, 1358.

(33) Schafer, A.; Horn, H.; Ahlrichs, R. *J. Chem. Phys.* **1992**, *97*, 2571.

(34) Hehre, W. J.; Ditchfield, R.; Pople, J. A. *J. Chem. Phys.* **1972**, *56*, 2257.

(35) Frisch, M. J.; Pople, J. A.; Binkley, J. S. *J. Chem. Phys.* **1984**, *80*, 3265.

(36) Curtiss, L. A.; Raghavachari, K. In *Computational Thermochemistry*; Irikura, K., Frurip, D., Eds.; American Chemical Society: Washington, DC, 1998; Vol. 677, p 176.

(37) Vondrak, T.; Wang, H.; Winget, P.; Cramer, C. J.; Zhu, X.-Y. To be published.